

Pointwise-in-time a posteriori error control for higher-order discretizations of time-fractional parabolic equations

Sebastian Franz* Natalia Kopteva†

January 27, 2023

Abstract

Time-fractional parabolic equations with a Caputo time derivative are considered. For such equations, we explore and further develop the new methodology of the a-posteriori error estimation and adaptive time stepping proposed in [10]. We improve the earlier time stepping algorithm based on this theory, and specifically address its stable and efficient implementation in the context of high-order methods. The considered methods include an L1-2 method and continuous collocation methods of arbitrary order, for which adaptive temporal meshes are shown to yield optimal convergence rates in the presence of solution singularities.

AMS subject classification (2010): 65M15

Key words: time-fractional, subdiffusion, a posteriori error estimation, adaptive time stepping algorithm, higher order, collocation, L1-2 method, stable implementation

1 Introduction

We address the numerical solution of fractional-order parabolic equations, of order $\alpha \in (0, 1)$, of the form

$$D_t^\alpha u + Lu = f(x, t) \quad \text{for } (x, t) \in \Omega \times (0, T], \quad (1)$$

subject to an initial condition $u(\cdot, 0) = u_0$ in Ω , and the boundary condition $u = 0$ on $\partial\Omega$ for $t > 0$. This problem is posed in a bounded Lipschitz domain $\Omega \subset \mathbb{R}^d$ (where $d \in \{1, 2, 3\}$), and involves a spatial linear second-order elliptic operator $L = L(t)$ of the form

$$Lu := - \sum_{i,j=1}^d \partial_{x_i} (a_{ij}(x, t) \partial_{x_j} u) + \sum_i^d b_i(x, t) \partial_{x_i} u + c(x, t) u, \quad (2)$$

*Institute of Scientific Computing, Technische Universität Dresden, Germany. e-mail: sebastian.franz@tu-dresden.de

†corr. author, Department of Mathematics and Statistics, University of Limerick, Ireland. e-mail: natalia.kopteva@ul.ie

with a symmetric positive definite coefficient matrix $\{a_{ij}(x, t)\}_{i,j=1}^d \forall (x, t) \in \Omega \times (0, T]$. The Caputo fractional derivative in time, denoted here by D_t^α , is defined [3], for $t > 0$, by

$$D_t^\alpha u := J_t^{1-\alpha}(\partial_t u), \quad J_t^{1-\alpha} v(\cdot, t) := \frac{1}{\Gamma(1-\alpha)} \int_0^t (t-s)^{-\alpha} v(\cdot, s) ds, \quad (3)$$

where $\Gamma(\cdot)$ is the Gamma function, and ∂_t denotes the partial derivative in t .

The purpose of this paper is to explore and further develop the new methodology of the a-posteriori error estimation and adaptive time stepping proposed in [10] (see also a recent extension of this approach in [12]). One distinctive feature of the present article is that we employ the approach of [10, 12] in a wider context, to wide classes of temporal discretizations for (1) of arbitrarily high order. In comparison, only the L1 method was considered in [10, 12], while now we also address an L1-2 method proposed in [5] and a family of continuous collocation methods of arbitrary order. It should be noted that despite a substantial literature on the a-priori error bounds for problem of type (1), both on uniform and graded temporal meshes—see, e.g., [6–8, 11, 13, 14, 16, 20] and references therein—the a-priori error analysis of the collocation methods appears very problematic on reasonably general meshes. The adaptive algorithm based on our theory, by contrast, yields reliable computed solutions and attains optimal convergence rates in the presence of solution singularities for all numerical approximations that we consider.

We also note an interesting alternative approach to the a-posteriori error estimation for problems of type (1) recently proposed in [1]; however, the latter approach has been tested mainly on a-priori chosen meshes, and it remains unclear how it may be implemented in an adaptive time stepping algorithm (in view of the nonlocal nature of the estimators).

To give a flavour of the advantages in the accuracy of numerical approximations offered by our adaptive approach, we compare the errors of 5 numerical methods on uniform temporal meshes (see Fig. 1 left) vs. adaptive meshes (Fig. 1 right), with a striking improvement in the accuracy due to the adaptive time stepping. Here we consider the L1 method, an L1-2 method from [5], and the continuous collocation methods of order 2, 4, and 8 (for details on the algorithm and the test problem, the reader is referred to Sections 5–6, in particular, Section 6.1). Overall, here and in Section 6, we observe that the algorithm is capable of adapting the time steps to the initial singularity, as well to solution spikes away from the initial time.

The main findings of the paper are as follows.

- The considered adaptive technology is reliable in the sense that it is based on theoretical pointwise-in-time a-posteriori error bounds. Importantly, our adaptive algorithm is essentially independent of the method (or its order) and, additionally, does not require a preliminary a-priori error analysis either of the exact solution or its numerical approximation. The latter may be important if the a-priori error analysis is lacking (such as for collocation methods) or limited to, e.g., uniform meshes.
- We demonstrate that high-order methods (of order up to as high as 8) exhibit a huge improvement in the accuracy when the time steps are chosen adaptively. In fact, our algorithm yields optimal convergence rates of order $q - \alpha$, where q denotes the order

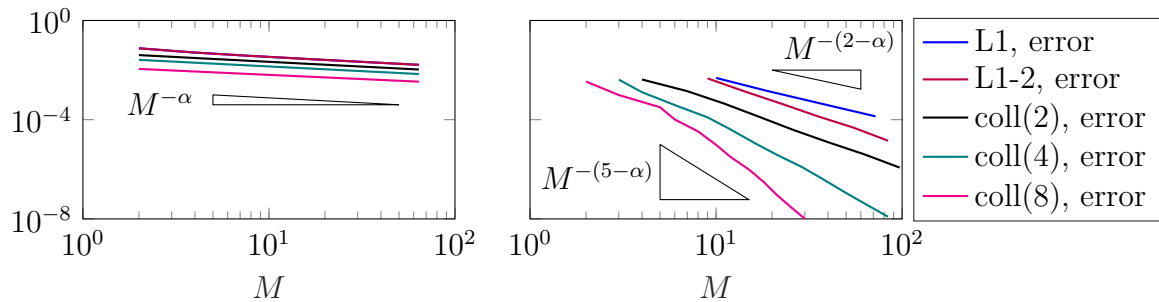


Figure 1: $L_\infty(0, T; L_\infty(\Omega))$ errors for various methods vs. number of time steps M for Example 6.1, $\alpha = 0.4$ on uniform meshes (left), and adaptive meshes (right) with residual barrier \mathcal{R}_0 , $\lambda = \pi^2$, and $\omega = \lambda/8$

of the method, either globally in time or in positive time (depending on the desired error profile used by the algorithm). At the same time, the algorithm is capable of capturing both initial singularities and local shocks/peaks in the solution.

- We make a few subtle improvements in the original version of the time stepping algorithm [10] that substantially reduce the computational time. In particular, we modify the choice and search for a suitable initial time step, and also numerically test the algorithm parameters.
- We provide clear and specific recommendations on the stable and efficient implementation of the resulting algorithm, which are essential, and not at all straightforward, in the context of higher-order methods. Hence, we obtain numerically stable and efficient implementations for all considered methods (including computations of their residuals) with α at least within the range between 0.1 and 0.999 and for values of TOL (used in the target bound for the error) as small as 10^{-8} .

The paper is organised as follows. In Section 2 we recall a posteriori error estimates from [10] and give a few generalizations, such as for the semilinear case. Next, in Section 3, we introduce numerical approximations for our problem (1) and describe the evaluation of their residuals (which are required by the algorithm). The computationally stable implementation of these methods, as well the stable computation of the residuals, is addressed in Section 4, while our adaptive algorithm is described in Section 5. Finally, in Section 6, we perform extensive numerical experiments to demonstrate the effectiveness and reliability of our adaptive approach.

Notation. We use the standard inner product $\langle \cdot, \cdot \rangle$ and the norm $\|\cdot\|$ in the space $L_2(\Omega)$, as well as the standard spaces $L_\infty(\Omega)$, $H_0^1(\Omega)$, $L_\infty(0, t; L_2(\Omega))$, and $W_\infty^1(t', t''; L_2(\Omega))$ (see [4, Section 5.9.2] for the notation used for functions of x and t). The notation $v^+ := \max\{0, v\}$ is used for the positive part of a generic function v .

2 A posteriori error estimates

We start by recalling a few results from [10] and then give a few generalizations, such as Lemma 2.5, which will allow for more efficient algorithms, and Corollary 2.12 for the semilinear case. Define the operator $(D_t^\alpha + \lambda)^{-1}$ by

$$(D_t^\alpha + \lambda)^{-1}v(t) := \int_0^t (t-s)^{\alpha-1} E_{\alpha,\alpha}(-\lambda[t-s]^\alpha) v(s) ds \quad \forall t > 0. \quad (4)$$

Here $E_{\alpha,\beta}(s) = \sum_{k=0}^{\infty} \{\Gamma(\alpha k + \beta)\}^{-1} s^k$ is a generalized Mittag-Leffler function. The notation $(D_t^\alpha + \lambda)^{-1}$ reflects [3, Remark 7.1] that (4) gives a solution w of the equation $(D_t^\alpha + \lambda)w(t) = v(t)$ for $t > 0$ subject to $w(0) = 0$.

Theorem 2.1 ([10, Theorem 2.2]). *Let L in (1), for some $\lambda \in \mathbb{R}$, satisfy $\langle Lv, v \rangle \geq \lambda \|v\|^2 \forall v \in H_0^1(\Omega)$. Suppose a unique solution u of (1) and its approximation u_h are in $C([0, T]; L_2(\Omega)) \cap W_\infty^1(\epsilon, t; L_2(\Omega))$ for any $0 < \epsilon < t \leq T$, and also in $H_0^1(\Omega)$ for any $t > 0$, while $u_h(\cdot, 0) = u_0$. Then the error of the latter is bounded in terms of its residual $R_h(\cdot, t) = (D_t^\alpha + L)u_h(\cdot, t) - f(\cdot, t)$ as follows:*

$$\|(u_h - u)(\cdot, t)\| \leq (D_t^\alpha + \lambda)^{-1} \|R_h(\cdot, t)\| \quad \forall t > 0. \quad (5)$$

Note that the key ingredient in the proof of the above result is the bound [10, Lemma 2.8]

$$\langle D_t^\alpha v(\cdot, t), v(\cdot, t) \rangle \geq (D_t^\alpha \|v(\cdot, t)\|) \|v(\cdot, t)\| \quad \forall t > 0,$$

valid for any $v \in L_\infty(0, t; L_2(\Omega)) \cap W_\infty^1(\epsilon, t; L_2(\Omega))$ for any $0 < \epsilon < t \leq T$, subject to $v(\cdot, 0) = 0$. Hence, one gets $(D_t^\alpha + \lambda) \|(u_h - u)(\cdot, t)\| \leq \|R_h(\cdot, t)\| \forall t > 0$, which then yields (5).

Furthermore, one gets a version of Theorem 2.1 for the $L_\infty(\Omega)$ norm.

Theorem 2.2 ([10, Theorem 3.2]). *Suppose that the coefficients of L in (1) are sufficiently smooth, and $c \geq \lambda$ for some $\lambda \in \mathbb{R}$. Let a unique solution u of (1) and its approximation u_h be in $C^2(\Omega)$ for each $t > 0$, and, for each $x \in \Omega$, belong to $W_\infty^1(\epsilon, t)$ for any $0 < \epsilon < t \leq T$, while $u_h(\cdot, 0) = u_0$. Then the error bound (5) of Theorem 2.1 remains true with $\|\cdot\| = \|\cdot\|_{L_2(\Omega)}$ replaced by $\|\cdot\|_{L_\infty(\Omega)}$.*

Remark 2.3. *Note that in [10], the above Theorem 2.2 was given for the case $\lambda \geq 0$ (and also for L without mixed derivatives). But in view of a more recent paper [9] addressing the maximum principle for the case of a reaction coefficient of arbitrary sign (see also [15] for a self-adjoint time-independent L), the proof in [10] also applies to this more general case.*

While Theorems 2.1 and 2.2 give computable a-posteriori error estimates on any given temporal mesh, it is not immediately clear how the time steps may be chosen adaptively to attain a certain solution accuracy, or, more ambitiously, a certain pointwise-in-time error profile. This is addressed by the next result, which is a version of [10, Corollary 2.3].

Corollary 2.4 (residual barrier). *Suppose that $p \in \{2, \infty\}$, and for some non-negative barrier function $\mathcal{E} \in W_\infty^1(\epsilon, t)$ for any $0 < \epsilon < t \leq T$, such that $\lim_{t \rightarrow 0^+} \mathcal{E}(t) \geq 0$ exists, one has*

$$\|R_h(\cdot, t)\|_{L_p(\Omega)} \leq (D_t^\alpha + \lambda)\mathcal{E}(t) \quad \forall t > 0. \quad (6)$$

Then, under the conditions of Theorem 2.1 if $p = 2$, and under the conditions of Theorem 2.2 if $p = \infty$, one has $\|(u_h - u)(\cdot, t)\|_{L_p(\Omega)} \leq \mathcal{E}(t) \forall t \geq 0$.

Possible choices of \mathcal{E} are discussed in Section 2.1. Note that while $\mathcal{E} \in W_\infty^1(\epsilon, t)$ for any $0 < \epsilon < t \leq T$ implies that $\mathcal{E} \in C(0, T]$, it is convenient to choose \mathcal{E} such that $\mathcal{E}(0) = 0$ and $\mathcal{E}(0^+) := \lim_{t \rightarrow 0^+} \mathcal{E}(t) > 0$, i.e. discontinuous at $t = 0$. (To be more precise, setting $\mathcal{E}(0) = 0$ yields the least restrictive barrier on the residual, while retaining $\mathcal{E}(t) \geq 0 \forall t \geq 0$ [10].)

Note that for some operators, such as $L = -\Delta = -\sum_{i=1}^d \partial_{x_i}^2$, Theorem 2.2 is applicable with $\lambda = 0$, while a negative reaction coefficient c in (2) would imply that $\lambda < 0$, which would limit the applicability of our results in Section 2.1. To rectify this, we now establish an improved version of Corollary 2.4 for $p = \infty$.

Lemma 2.5 (improved residual barrier for $L_\infty(\Omega)$). *Suppose that for $\lambda, \omega \in \mathbb{R}$, where $\omega \geq 0$, there exists a function $g \in C^2(\Omega)$ such that $Lg \geq \lambda$ and $1 \leq g \leq 1 + \omega$ in Ω (if $L = L(t)$, then $L(t)g \geq \lambda \forall t > 0$). Also, suppose that for some non-negative barrier function $\mathcal{E} \in W_\infty^1(\epsilon, t)$ for any $0 < \epsilon < t \leq T$, such that $\lim_{t \rightarrow 0^+} \mathcal{E}(t) \geq 0$ exists and $\omega D_t^\alpha \mathcal{E}(t) \geq 0 \forall t > 0$, one has*

$$\|R_h(\cdot, t)\|_{L_\infty} \leq \frac{(D_t^\alpha + \lambda)\mathcal{E}(t)}{1 + \omega} \quad \forall t > 0. \quad (7)$$

Then, under the conditions of Theorem 2.1, one has $\|(u_h - u)(\cdot, t)\|_{L_\infty} \leq \mathcal{E}(t) \forall t \geq 0$.

Proof. Set $\hat{\mathcal{E}}(x, t) := g(x)\mathcal{E}(t)$. Then $D_t^\alpha \hat{\mathcal{E}} = gD_t^\alpha \mathcal{E} \geq D_t^\alpha \mathcal{E}$ (in view of $(1 - g)D_t^\alpha \mathcal{E} \geq 0$ whether $\omega = 0$ or $\omega > 0$), so

$$(D_t^\alpha + L)\hat{\mathcal{E}}(x, t) \geq (D_t^\alpha + \lambda)\mathcal{E}(t) \geq (1 + \omega)|R_h(x, t)| = (1 + \omega)|(D_t^\alpha + L)(u_h - u)(x, t)|.$$

Now, an application of the maximum principle for the operator $D_t^\alpha + L$ (see, e.g., [9]) yields

$$(1 + \omega)|(u_h - u)(x, t)| \leq \hat{\mathcal{E}}(x, t) = g(x)\mathcal{E}(t) \leq (1 + \omega)\mathcal{E}(t).$$

This immediately implies (7). □

Remark 2.6 (λ and ω in Lemma 2.5). *(i) Setting $\omega := 0$ and $g := 1$ in Lemma 2.5 immediately yields Corollary 2.4 for $p = \infty$ with $\lambda := \inf_{\Omega \times (0, T)} c$.*

(ii) If $c \geq 0$, for any $\lambda > 0$, one may choose g such that $Lg = \max\{\lambda, c\}$ in Ω , subject to $g = 1$ on $\partial\Omega$, and $1 + \omega := \sup_\Omega g$ (then $L(g - 1) \geq 0$, so, by the maximum principle, $g \geq 1$). For example, if $\Omega = (0, 1)$ and $L := -\partial_x^2$, then $g = 1 + \frac{1}{2}\lambda x(1 - x)$ yields $\omega = \frac{1}{8}\lambda$ for any $\lambda \geq 0$. For the same L on a more general $\Omega = (0, \bar{x})$ one similarly gets $g = 1 + \frac{1}{2}\lambda x(\bar{x} - x)$, so $\omega = \frac{1}{8}\lambda \bar{x}^2$ for any $\lambda \geq 0$.

(iii) Even if $c < 0$, in some cases one may still use Lemma 2.5 with positive λ and ω . For example, if $\Omega = (0, 1)$ and $L := -\partial_x^2 - c_0$ for some constant $0 < c_0 < 8$, then $g = 1 + 4\omega x(1 - x) \leq 1 + \omega$ yields $Lg \geq 8\omega - c_0(1 + \omega) =: \lambda$. So for any $\lambda > 0$, we can choose $\omega = \omega(\lambda)$ to be used in (7).

Remark 2.7 (flexibility of (7) vs. (6)). *It may appear that the new residual barrier (7) is more restrictive compared to (6). In fact, (7) is not only more general (as it reduces to (6) in a particular case of $\omega = 0$). Importantly, by allowing larger values of λ , (7) weakens the restriction on the residual (albeit with an additional factor $(1 + \omega)^{-1}$). This additional flexibility allows for more efficient time stepping algorithms.*

2.1 Residual profiles for $\lambda \geq 0$

Corollary 2.4 seems to imply that there is abundant flexibility in the choice of a desirable pointwise-in-time error profile $\mathcal{E}(t)$. However, one needs to ensure that the non-local inequality $(D_t^\alpha + \lambda)\mathcal{E}(t) > 0$ holds true $\forall t > 0$. Furthermore, one should avoid a positive $(D_t^\alpha + \lambda)\mathcal{E}(t)$ becoming too small at any time $t = t^* > 0$, as the latter, combined with a suitable adaptive time stepping algorithm attempting to attain (6), may lead to the local time step near t^* becoming unpractically small, or, even worse, the adaptive algorithm failing to satisfy the required bound (6) (as R_h is also non-local).

The following lemma describes two possible error profiles, which are motivated by the pointwise-in-time a-priori error analyses [8, 11]; see also a discussion in Remark 2.10.

Lemma 2.8 ([10, Corollary 2.4]). *Suppose that $p \in \{2, \infty\}$ and $\lambda \geq 0$. Then, under the conditions of Theorem 2.1 if $p = 2$, and under the conditions of Theorem 2.2 if $p = \infty$, for the error $e = u_h - u$ one has*

$$\|e(\cdot, t)\|_{L_p(\Omega)} \leq \sup_{0 < s \leq t} \left\{ \frac{\|R_h(\cdot, s)\|_{L_p(\Omega)}}{\mathcal{R}_0(s)} \right\}, \quad \mathcal{R}_0(t) := \{\Gamma(1 - \alpha)\}^{-1} t^{-\alpha} + \lambda, \quad (8a)$$

$$\|e(\cdot, t)\|_{L_p(\Omega)} \leq t^{\alpha-1} \sup_{0 < s \leq t} \left\{ \frac{\|R_h(\cdot, s)\|_{L_p(\Omega)}}{\mathcal{R}_1(s)} \right\}, \quad \mathcal{R}_1(t) := \{\Gamma(1 - \alpha)\}^{-1} t^{-1} \rho(\tau/t) + \lambda \mathcal{E}_1(t), \quad (8b)$$

$$\mathcal{E}_1(t) := \max\{\tau, t\}^{\alpha-1}, \quad \rho(s) := s^{-\beta} [1 - ((1 - s)^+)^{\beta}], \quad \beta := 1 - \alpha, \quad (8c)$$

where $\tau > 0$ is an arbitrary parameter (and $t^{\alpha-1}$ in (8b) can be replaced by $\mathcal{E}_1(t)$).

The above lemma may be reformulated for the purpose of a possible adaptive time stepping algorithm with some desirably small positive TOL , as follows:

$$\|R_h(\cdot, t)\|_{L_p(\Omega)} \leq TOL \cdot \mathcal{R}_0(t) \quad \forall t > 0 \quad \Rightarrow \quad \|e(\cdot, t)\|_{L_p(\Omega)} \leq TOL, \quad (9a)$$

$$\|R_h(\cdot, t)\|_{L_p(\Omega)} \leq TOL \cdot \mathcal{R}_1(t) \quad \forall t > 0 \quad \Rightarrow \quad \|e(\cdot, t)\|_{L_p(\Omega)} \leq TOL \cdot t^{\alpha-1}. \quad (9b)$$

Hence, $\|R_h(\cdot, t)\|_{L_p(\Omega)} \leq TOL \cdot \mathcal{R}_l(t)$, with $l \in \{0, 1\}$ and $p \in \{2, \infty\}$, can be employed as a criterion for the adaptive time stepping (see Section 5 for further details on such algorithms). Furthermore, an inspection of the proof of Lemma 2.8 (given in [10]) shows that under the conditions of Lemma 2.5 one immediately gets more general versions of (9a) and (9b) for $p = \infty$; see below. These new versions are of interest since they are valid for possibly larger values of λ in the definitions of $\mathcal{R}_0(t)$ and $\mathcal{R}_1(t)$ (see Remarks 2.6 and 2.7).

Corollary 2.9. *Under the conditions of Lemma 2.5, for the error $e = u_h - u$, one has*

$$\|R_h(\cdot, t)\|_{L_\infty(\Omega)} \leq \frac{TOL \cdot \mathcal{R}_0(t)}{1 + \omega} \quad \forall t > 0 \quad \Rightarrow \quad \|e(\cdot, t)\|_{L_\infty(\Omega)} \leq TOL, \quad (10a)$$

$$\|R_h(\cdot, t)\|_{L_\infty(\Omega)} \leq \frac{TOL \cdot \mathcal{R}_1(t)}{1 + \omega} \quad \forall t > 0 \quad \Rightarrow \quad \|e(\cdot, t)\|_{L_\infty(\Omega)} \leq TOL \cdot t^{\alpha-1}. \quad (10b)$$

Remark 2.10 (error profiles v pointwise a-priori error bounds). *Suppose that u exhibits an initial singularity of type t^α , typical for this problem, with the derivative bounds $\|\partial_t^l u(\cdot, t)\|_{L_p(\Omega)} \leq Ct^{\alpha-l} \forall t > 0, 1 \leq l \leq q$, with some integer $q \geq 2$, constant $C > 0$, and $p \in \{2, \infty\}$. Then the error bounds of type [11, (3.2)] and [8, (4.2)] imply that given a method of order q on a graded mesh $\{T(j/M)^r\}_{j=0}^M$ (with $q = 2$ for the L1 method), depending on the degree of grading, the error is either proportional to $t^{\alpha-1}$ or (if the grading parameter r exceeds $q - \alpha$) to $t^{\alpha-(q-\alpha)/r}$. Hence, the two error profiles of interest that we consider are proportional to $\mathcal{E}_0(t) = 1$ for $t > 0$, or $\mathcal{E}_1(t) = t^{\alpha-1}$ for $t > \tau > 0$; see (9a) and (9b), respectively. (To be more precise, $\mathcal{E}_1(t) := \max\{\tau, t\}^{\alpha-1}$, while $\mathcal{E}_0(0) = \mathcal{E}_1(0) = 0$. In fact, \mathcal{R}_0 and \mathcal{R}_1 in (8) and, hence, (9) are obtained simply by an application of $D_t^\alpha + \lambda$ to respectively \mathcal{E}_0 and \mathcal{E}_1 [10].)*

With these two choices, the a-priori error bounds from [8, 11] suggest that the error is expected to be respectively $\lesssim M^{q-\alpha}$ or $\lesssim M^{q-\alpha}t^{\alpha-1} \forall t \in [0, T]$, which agrees, and surprisingly well, with numerical results in Section 6.1. Note also that these convergence rates are consistent with those in [8, 11] on a-priori chosen graded meshes with $r = (q - \alpha)/\alpha$ and $r = 2 - \alpha$, respectively (in the latter case, up to the logarithmic term $\ln M$).

Remark 2.11 ($\lambda < 0$). *Strictly speaking, Lemma 2.8 also applies to the case $\lambda < 0$. However, in this case both \mathcal{R}_0 and \mathcal{R}_1 become negative at some $t > 0$, so the residual bound $\|R_h(\cdot, s)\|_{L_p(\Omega)} \leq TOL \cdot \mathcal{R}_l(t)$ (with $l = 0, 1$) cannot be attained. One possible remedy is to replace \mathcal{R}_l by $\mathcal{R}_l^* := \max\{\mathcal{R}_l, \varepsilon\}$ with some small parameter ε , in which case the error will be bounded by $TOL \cdot \mathcal{E}^*(t)$, where $\mathcal{E}^* := (D_t^\alpha + \lambda)^{-1}\mathcal{R}_l^*$. Clearly, one will enjoy $\mathcal{E}^* = \mathcal{E}_l$ for $t \leq t^*$ as long as $\mathcal{R}_l^* = \mathcal{R}_l \forall t \in (0, t^*]$. Afterwards \mathcal{E}^* may be computed with sufficiently high accuracy by solving the fractional ODE $(D_t^\alpha + \lambda)\mathcal{E}^* = \mathcal{R}^*$ numerically on a very fine mesh.*

2.2 Generalization for the semilinear case

One can easily extend the above results to the following semilinear version of (1):

$$D_t^\alpha u + Lu + g(x, t, u) = f(x, t) \quad \text{for } (x, t) \in \Omega \times (0, T], \quad (11)$$

assuming that g is sufficiently smooth and, with some $\mu \in \mathbb{R}$, satisfies

$$\partial_v g(x, t, v) \geq \mu \quad \forall (x, t, v) \in \Omega \times (0, T] \times \mathbb{R}.$$

Then, in view of the standard linearization

$$g(x, t, u_h) - g(x, t, u) = \hat{c}(x, t)(u_h - u), \quad \hat{c} := \int_0^1 \partial_v g(x, t, u + s(u_h - u)) ds \geq \mu,$$

the error satisfies $(D_t^\alpha + L + \hat{c})(u_h - u) = R_h$, with the updated definition of the residual

$$R_h := D_t^\alpha u_h + Lu_h + g(x, t, u_h) - f(x, t).$$

Corollary 2.12 (semilinear case). *Assume that $\langle Lv, v \rangle \geq \lambda^* \|v\|^2$ in Theorem 2.1 for some $\lambda^* \in \mathbb{R}$ (instead of $\langle Lv, v \rangle \geq \lambda \|v\|^2$), or, similarly, $c \geq \lambda^*$ in Theorem 2.2 (instead of $c \geq \lambda$). Then one gets the error bound (5) with $\lambda := \lambda^* + \mu$. In the latter $\|\cdot\|$ is understood as $\|\cdot\|_{L_p(\Omega)}$ with $p = 2$ or $p = \infty$, respectively. A version of Corollary 2.4, as well as a version of Lemma 2.8, is also valid for the semilinear equation (11).*

3 Numerical approximations and their residuals

In this Section we describe several numerical approximations for our time-fractional problem (1) and also discuss the evaluation of their residuals (the latter are to be used by the adaptive algorithm considered in Section 5). All numerical methods are presented relative to an arbitrary temporal mesh $\{t_k\}_{k=0}^M$ covering $[0, T]$ with intervals $(t_{k-1}, t_k]$ of width τ_k , and are conveniently described using certain continuous piecewise-polynomial functions in time.

3.1 L1 method

We start with the popular L1 method; see, e.g., [6, 19] and references therein. Defining the numerical approximation u_h in $\bar{\Omega} \times [0, T]$ as continuous piecewise-linear in time, one can describe the L1 method by

$$(D_t^\alpha + L) u_h(x, t_k) = f(x, t_k) \quad \text{for } x \in \Omega, \quad k = 1, \dots, M, \quad (12)$$

subject to $u_h^0 := u_0$ and $u_h = 0$ on $\partial\Omega$.

To be more precise, with the notation $U_k := u_h(\cdot, t_k)$,

$$u_h(t)|_{[t_{k-1}, t_k]} := U_{k-1} \phi_k^0(t) + U_k \phi_k^1(t),$$

where

$$\phi_k^0(t) := \frac{t_k - t}{\tau_k}, \quad \phi_k^1(t) := \frac{t - t_{k-1}}{\tau_k} = 1 - \phi_k^0(t). \quad (13)$$

To implement the L1 method, one needs to evaluate the non-local $D_t^\alpha u_h(\cdot, t_k)$ in terms of $\{U_k\}$. More generally, to compute the residual R_h (to be used by the adaptive algorithm), one needs to compute $D_t^\alpha u_h(\cdot, t)$ for any $t > 0$. For $t_{k-1} < t \leq t_k \forall k \geq 1$, a straightforward calculation using (3) yields

$$D_t^\alpha u_h(t) = \frac{1}{\Gamma(2 - \alpha)} \left(- \sum_{j=1}^{k-1} \frac{U_j - U_{j-1}}{\tau_j} (t - s)^{1-\alpha} \Big|_{s=t_{j-1}}^{s=t_j} + \frac{U_k - U_{k-1}}{\tau_k} (t - t_{k-1})^{1-\alpha} \right). \quad (14)$$

Stable implementations of this method, as well as the other considered methods, will be discussed in Section 4, while the efficient computation of the residuals for all considered methods will be addressed in Section 3.4.

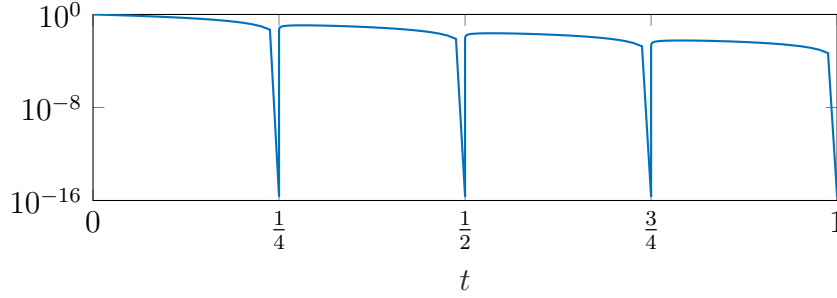


Figure 2: The residual $\|R_h\|_{L^\infty(\Omega)}$ of the L1-method for problem (1) with $\alpha = 0.8$, $L = -\Delta$, $f = 1 + t$, $\Omega = (0, 1)$, $u_0 = 0$.

For the latter, note that (12) immediately implies for the residual that $R_h(\cdot, t_k) = 0$ for $k \geq 1$; hence on each (t_{k-1}, t_k) for $k > 1$, the residual is a non-symmetric bubble. This is illustrated by Figure 2, which shows a typical behaviour for the residual of the L1-method on an equidistant temporal mesh of four cells.

3.2 L1-2 method

A natural improvement over the L1-method is to use a piecewise quadratic u_h . Assuming the associated degrees of freedom are $\{U_k = u_h(\cdot, t_k)\}_{k=0}^M$, there are several possibilities of defining such a method; see, e.g., [8, 16]. We will use an alternative method proposed in [5] as it employs a more natural (backward quadratic) interpolation of the computed solution between time layers, which allows for a simpler evaluation of the residuals (see a discussion in Section 3.4). Note that, in contrast with [8, 16], we are not aware of any a-priori error analysis for the L1-2 method of [5]; nevertheless, our a-posteriori error analysis applies seamlessly to this method.

Let u_h be continuous in time, linear on the first interval $[0, t_1]$, and piecewise-quadratic on $[t_1, T]$ as follows:

$$\begin{aligned} u_h(t)|_{[0, t_1]} &:= U_0 \phi_1^0(t) + U_1 \phi_1^1(t), \\ u_h(t)|_{[t_{k-1}, t_k]} &:= U_{k-1} \phi_k^0(t) + U_k \phi_k^1(t) + y_k \phi_k^2(t) \quad \forall k \geq 2. \end{aligned}$$

Here

$$y_k := \frac{\frac{U_k - U_{k-1}}{\tau_k} - \frac{U_{k-1} - U_{k-2}}{\tau_{k-1}}}{\tau_k + \tau_{k-1}},$$

while ϕ_k^0 and ϕ_k^1 are from (13), and

$$\phi_k^2(t) := (t - t_{k-1})(t - t_k).$$

With the above piecewise-quadratic u_h , the L1-2 method of [5] can be described, similarly to the L1 method, by (12). Hence, for the residual one again gets $R_h(\cdot, t_k) = 0$ for $k \geq 1$, i.e. the residual remains a non-symmetric bubble on each (t_{k-1}, t_k) for $k > 1$. Figure 3 shows a

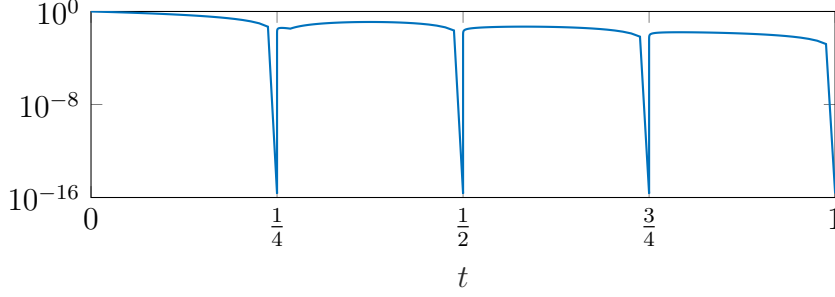


Figure 3: Typical behaviour of the residual of the L1-2 method (shown in the same setting as in Figure 2).

typical behaviour for the residuals of the L1-2 method on an equidistant mesh of four cells.

To implement this method, one needs to reevaluate $D_t^\alpha u_h(\cdot, t_k)$, while to compute the residual R_h , one, more generally, needs to compute the non-local $D_t^\alpha u_h(\cdot, t)$ for any $t > 0$. For the first time interval, i.e. for $0 < t \leq t_1$ we recall (14), which simplifies to

$$D_t^\alpha u_h(t) = \frac{1}{\Gamma(2-\alpha)} \frac{U_1 - U_0}{\tau_1} t^{1-\alpha}.$$

For $t_{k-1} < t \leq t_k \forall k \geq 2$, a more elaborate calculation using (3) yields

$$\begin{aligned} D_t^\alpha u_h(t) = & \frac{1}{\Gamma(2-\alpha)} \left(- \sum_{j=1}^{k-1} \frac{U_j - U_{j-1}}{\tau_j} (t-s)^{1-\alpha} \Big|_{t_{j-1}}^{t_j} + \frac{U_k - U_{k-1}}{\tau_k} (t-t_{k-1})^{1-\alpha} \right) \\ & + \frac{1}{\Gamma(1-\alpha)} \sum_{j=2}^{k-1} y_j \left(\frac{2}{2-\alpha} (t-s)^{2-\alpha} \Big|_{t_{j-1}}^{t_j} - \frac{2t-t_{j-1}-t_j}{1-\alpha} (t-s)^{1-\alpha} \Big|_{t_{j-1}}^{t_j} \right) \\ & + \frac{1}{\Gamma(1-\alpha)} y_k \left(- \frac{2}{2-\alpha} (t-t_{k-1})^{2-\alpha} + \frac{2t-t_{k-1}-t_k}{1-\alpha} (t-t_{k-1})^{1-\alpha} \right). \end{aligned}$$

3.3 Continuous collocation methods

To define higher-order methods, it is convenient to define computed solutions u_h as piecewise polynomials of higher degrees within the framework of continuous collocation methods; see, e.g., [2]. Note that we are not aware of any a-priori error analysis for high-order collocation methods in the context of time-fractional parabolic equation (1); nevertheless, our a-posteriori error analysis and our adaptive algorithm are immediately applicable to such methods, as is also demonstrated by numerical experiments in Section 6. A word of caution should be added: one needs to ensure a stable implementation of the method itself and of the adaptive time stepping algorithm. While a careful implementation is essential even for the L1 method, higher-order methods particularly require a more sophisticated treatment; see Sections 3.4 and 4 for further discussion.

Let u_h be a piecewise polynomial of degree $m \geq 1$, defined on a subgrid of collocation points $\{t_k^\ell\}_{\ell \in \{0, \dots, m\}}$ on each time interval $[t_{k-1}, t_k]$ with $t_k^\ell := t_{k-1} + c_\ell \cdot (t_k - t_{k-1})$, $\{c_\ell\} \subset [0, 1]$,

$c_0 = 0$, and $c_m = 1$. While the choice of the collocation points is quite arbitrary, in our experiments we shall simply use equidistant points.

Now, with any set $\{\phi_k^\ell\}$ of basis functions of $\mathcal{P}_m(t_{k-1}, t_k)$, the polynomial space of degree m over $[t_{k-1}, t_k]$, on which, for convenience, we impose

$$\phi_k^\ell(t_k^0) = \phi_k^\ell(t_{k-1}) = \delta_{\ell,0} \quad \text{and} \quad \phi_k^\ell(t_k^m) = \phi_k^\ell(t_k) = \delta_{\ell,m} \quad \forall \ell \in \{0, \dots, m\}, \quad (15)$$

let

$$u_h(t)|_{(t_{k-1}, t_k)} = \sum_{\ell=0}^m U_k^\ell \phi_k^\ell(t) = U_{k-1}^m \phi_k^0(t) + \sum_{\ell=1}^m U_k^\ell \phi_k^\ell(t).$$

Here, in agreement with (15), $U_k^0 := u_h(\cdot, t_{k-1})$ and $U_k^m := u_h(\cdot, t_k)$, and we additionally impose the continuity of u_h in time, which is equivalent to $U_{k-1}^m = U_k^0$, while $U_0^m := U_1^0$.

With the above definitions, a continuous collocation method is given by

$$(D_t^\alpha + L) u_h(x, t_k^\ell) = f(x, t_k^\ell) \quad \text{for } x \in \Omega, \ell \in \{1, \dots, m\}, k = 1 \dots, M, \quad (16)$$

subject to $u_h^0 := u_0$ and $u_h = 0$ on $\partial\Omega$. A comparison with (12) shows that for $m = 1$ the above collocation method is identical with the L1 method.

To implement the above method, one needs to evaluate $D_t^\alpha u_h(\cdot, t_k^\ell)$, while to compute the residual, one requires a more general $D_t^\alpha u_h(\cdot, t)$. For the latter, for $t_{k-1} < t \leq t_k \forall k \geq 1$, one gets

$$D_t^\alpha u_h(t) = \frac{1}{\Gamma(1-\alpha)} \left(\sum_{j=1}^{k-1} \int_{t_{j-1}}^{t_j} \left[U_{j-1}^m \partial \phi_j^0(s) + \sum_{\ell=1}^m U_j^\ell \partial \phi_j^\ell(s) \right] (t-s)^{-\alpha} ds + \int_{t_{k-1}}^t \left[U_{k-1}^m \partial \phi_k^0(s) + \sum_{\ell=1}^m U_k^\ell \partial \phi_k^\ell(s) \right] (t-s)^{-\alpha} ds \right). \quad (17)$$

A stable implementation of this formula will be discussed in the Section 4.

Thus, to implement the collocation method (16), on each time interval $(t_{k-1}, t_k]$ one needs to solve a linear system in $\{U_k^\ell\}_{\ell=1}^m$; the right-hand side of this linear system is computed using the values of u_h for $t \leq t_{k-1}$.

Note that the definition of the method (16) immediately implies that $R_h(\cdot, t_k^\ell) = 0$, i.e. the residual vanishes at all collocation points, except for $t = 0$. A typical behaviour of the residuals is illustrated in Figure 4. Importantly, in view of the bubble nature of the residuals, when computing the residual R_h , one should employ sufficiently many well distributed sampling points between any two consecutive collocation points. For example, in our experiments we have used 20 sampling points per time interval; see also Figure 5.

3.4 Computation of the residuals. Discussion of alternative discretizations

Recall that the residuals of all considered methods exhibit a bubble-type behaviour. More formally, let R_h^t be the continuous piecewise-polynomial interpolant of R_h in time, defined

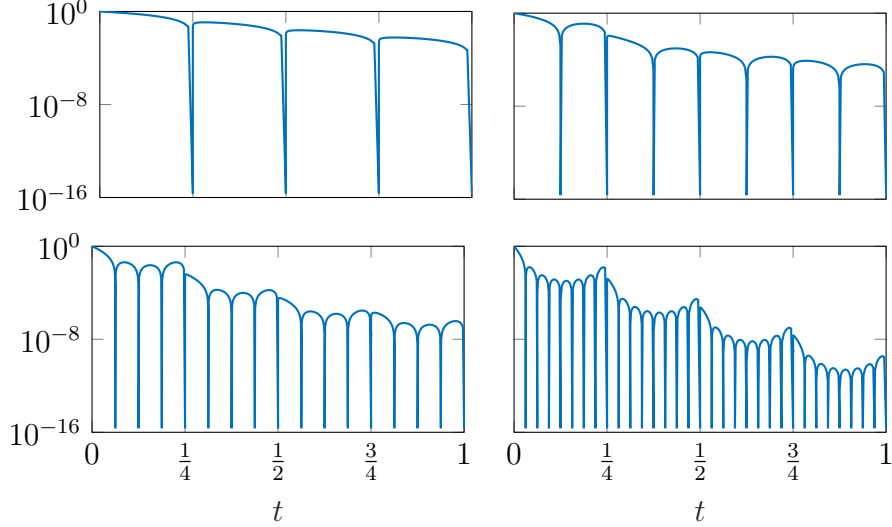


Figure 4: Typical behaviour of the residuals of collocation methods on an equidistant temporal mesh of four cells for $m \in \{1, 2, 4, 8\}$ from top left to bottom right (shown in the same setting as in Figure 2).

using exactly the same interpolation points and definitions as used for the corresponding computed solution u_h . Then the definitions of the above methods immediately imply that $R_h^I(t) = 0$ for $t \geq t_1$. More generally, for the L1 and L1-2 methods, note that $D_t^\alpha u_h^0(\cdot, 0) = 0$ (as u_h is linear on the first time interval); so $R_h(\cdot, 0) = Lu_0 - f(\cdot, 0)$ implies that $R_h^I(t) = [Lu_0 - f(\cdot, 0)](1 - t/t_1)^+$ for $t > 0$. For the considered collocation methods with $m > 1$, one additionally has $R_h^I(t_1^\ell) = 0$ at all interior collocation points over the first time interval, so $R_h^I(t) = R_h^I(\cdot, 0) \varphi_1^0(t)$ for $t > 0$, where $\varphi_1^0 \in \mathcal{P}_m(0, t_1)$, subject to $\varphi_1^0(t_1^\ell) = \delta_{0,\ell} \forall \ell = 0, \dots, m$ (i.e., in general, φ_1^0 may be different from ϕ_1^0 in (15)), and φ_1^0 vanishes for $t \geq t_1$.

Now, suppose that the spatial operator L in (1) is time-independent. Then $(Lu_h)^I = L(u_h)^I = Lu_h$ implies $R_h - R_h^I = (D_t^\alpha u_h - f) - (D_t^\alpha u_h - f)^I$. Hence, R_h can be computed by sampling, using parallel/vector evaluations and without a direct application of L (or its discrete version) to u_h .

Next, suppose that $L = L(t)$ in (1). Then $R_h - R_h^I$ includes an additional ingredient $Lu_h - (Lu_h)^I$, which can also be approximated by sampling, but with fewer points. For example, for the L1 method, $(Lu_h)^I$ is linear on each time interval (t_{k-1}, t_k) and equal to Lu_h at the end points. Depending on the coefficients of $L(t)$, a quadratic approximation may be adequate for Lu_h , in which case only one sample point per time interval will be required for this term.

Finally, note that some discretizations of D_t^α do not naturally lead to residuals vanishing at the nodes of the temporal mesh. Recall, for example, the alternative L2 method considered in [8, 16]. For the latter, assuming that L is time-independent, one still enjoys $R_h - R_h^I = (D_t^\alpha u_h - f) - (D_t^\alpha u_h - f)^I$. Although now R_h^I does not vanish at the mesh nodes, while the values of $R_h(\cdot, t_k)$ (required to compute R_h^I) involve $Lu_h(\cdot, t_k)$, the latter can be computed from the definition of the numeral method without a single additional application of L to the computed solution.

Another popular discretization that we do not consider in this paper is Alikhanov's L2-1 $_{\sigma}$ scheme (described, e.g., in [11, Section 4]). Recall that this scheme is similar to the above L2 methods with the main difference in that, when computing $u_h(\cdot, t_k)$, one assumes that u_h is piecewise-quadratic on $(0, t_{k-1})$ and linear on (t_{k-1}, t_k) , while the higher-order accuracy is ensured by replacing (12) with $(D_t^\alpha + L) u_h(x, t_k^*) = f(x, t_k^*)$, where $t_k^* := t_k - \frac{1}{2}\alpha\tau_k$. Despite u_h being linear in time on (t_{k-1}, t_k) , this choice of t_k^* yields higher-order accuracy of order $3 - \alpha$ at $t = t_k$. Consequently, the general error estimation methodology still applies, but for various a-posteriori error estimates of type (5) to remain sharp, an appropriate quadratic reconstruction of u_h is to be used on (t_{k-1}, t_k) .

More generally, our error estimation methodology is applicable to essentially any continuous-in-time computed solution independently of the method (the continuity in time, while being formally required by Theorems 2.1 and 2.2, is essential for bounded residuals). As such, it is also applicable for discontinuous collocation discretizations [2, p.84] and discontinuous Galerkin methods [17], once an appropriate continuous-in-time reconstruction of the computed solution is generated (see, e.g., [17, Section 6]) and used as $u_h(\cdot, t)$. A further numerical study in this direction is certainly warranted and will be presented elsewhere.

4 Computationally stable implementation

Note that the above formulas for $D_t^\alpha u_h(t)$, such as (14) for the L1 method, are used both in the implementation of the considered method itself and the computation of relevant residuals. A direct implementation of such formulas using exact integration generally yields numerically unstable solutions. In this Section, we will comment on some useful improvements that can be attained using certain reformulations.

- Hence, we obtain numerically stable and efficient implementations for all considered methods (including computations of their residuals) with α at least within the range between 0.1 and 0.999 and for values of TOL as small as 10^{-8} .

Such improvements will be described here by means of MatLab commands, while similar strategies may be employed in all other scientific programming languages. In particular, we rely on the two MatLab commands, `expm1` and `log1p`, which, being mathematically equivalent to

$$\text{expm1}(s) = \exp(s) - 1, \quad \text{log1p}(s) = \ln(1 + s), \quad (18)$$

are used for a more robust evaluation near $s = 0$.

Other possible strategies include higher-precision computations (e.g., with Multiprecision Computing Toolbox for MatLab used in [6]) and adaptive quadrature routines. In fact, for higher-order methods, we shall combine (18) with an adaptive quadrature rule in the form of MatLab function `integral` (which employs adaptive quadrature using a 7-point Gauß with an 15-point Kronrod-quadrature rule to vector-valued functions; see [18]).

However, the reader should be cautioned against applying adaptive quadrature routines to directly compute integrals in (14) or (17) (in view of singular integrals over (t_{k-1}, t) , as well as over (t_{j-1}, t_j) when the sampling point $t \approx t_j$). For example, a simple computational test

shows that, despite its versatility, `integral` becomes appallingly inaccurate when applied to a simple singular integral $\int_0^1 s^{-\alpha} ds$ as $\alpha \rightarrow 1^-$.

L1 method

The reason for numerical instabilities can be easily understood by examining the explicit formula (14) for $D_t^\alpha u_h$ of the simplest L1 method. The latter formula involves the evaluation of $(t-s)^{1-\alpha}|_{t_{j-1}}^{t_j}$, i.e. the difference of two nearly equal numbers (assuming that $(t-t_j) \approx (t-t_{j-1})$), which leads to noticeable round-off errors. The following simple reformulation using (18) immediately rectifies this instability. For $t > t_j$, set

$$d_j(t) := t - t_j, \quad \kappa_j(t) := \ln \left(\frac{d_j(t)}{d_{j-1}(t)} \right) = \text{log1p} \left(-\frac{\tau_j}{t - t_{j-1}} \right).$$

Now one gets

$$\begin{aligned} (t-s)^{1-\alpha}|_{t_{j-1}}^{t_j} &= d_j(t)^{1-\alpha} - d_{j-1}(t)^{1-\alpha} = d_{j-1}(t)^{1-\alpha} \left(\left(\frac{d_j(t)}{d_{j-1}(t)} \right)^{1-\alpha} - 1 \right) \\ &= d_{j-1}(t)^{1-\alpha} \text{expm1}((1-\alpha)\kappa_j(t)). \end{aligned} \quad (19)$$

Thus, (14), for $t_{k-1} < t \leq t_k$, allows a computationally stable reformulation

$$\begin{aligned} D_t^\alpha u_h(t) &= \\ &= \frac{1}{\Gamma(2-\alpha)} \left(-\sum_{j=1}^{k-1} \frac{U_j - U_{j-1}}{\tau_j} d_{j-1}(t)^{1-\alpha} \text{expm1}((1-\alpha)\kappa_j(t)) + \frac{U_k - U_{k-1}}{\tau_k} d_{k-1}(t)^{1-\alpha} \right). \end{aligned} \quad (20)$$

One may worry that, due to the summation, each U_j for $j < k$ is still multiplied by a difference of two possibly close numbers. Nevertheless, we observed stable performance of the above reformulation in all our experiments.

Higher-order methods. Adaptive quadrature

Numerical instabilities become even more intractable in the context of higher-order methods, and even more so since the higher accuracy, offered by such methods, is availed only if the computations are performed with higher precision. Below we shall describe a stable implementation for the collocation methods of arbitrary order m . Note that for $m = 1$, this approach reduces to the above (20). We also used a version of this approach for a stable implementation of the L1-2 method.

For the collocation methods, recall that (17) for $D_t^\alpha u_h(t)$, where $t_j \leq t_{k-1} < t \leq t_k$, involves the integrals of two types:

$$I_{hist}^{j,\ell} := \int_{t_{j-1}}^{t_j} \partial \phi_j^\ell(s) (t-s)^{-\alpha} ds \quad \text{and} \quad I_{sing}^\ell := \int_{t_{k-1}}^t \partial \phi_k^\ell(s) (t-s)^{-\alpha} ds, \quad \ell \in \{0, \dots, m\},$$

which we shall respectively refer to as the history integrals and the singular integrals.

It is convenient to describe a set of basis functions $\{\phi_j^\ell\}_{\ell \in \{0, \dots, m\}}$ on each $[t_{j-1}, t_j]$ using the reference interval $[0, 1]$ by

$$\phi_j^\ell(s) = \psi^\ell\left(\frac{s - t_{j-1}}{\tau_j}\right) =: \psi^\ell(\sigma), \quad \ell \in \{0, \dots, m\}. \quad (21)$$

Here, in agreement with (15), we also impose $\psi^\ell(0) = \delta_{\ell,0}$ and $\psi^\ell(1) = \delta_{\ell,m}$.

In the case of the L1 method (which corresponds to $m = 1$), the history integrals led to a possibly unstable evaluation of $(t - s)^{1-\alpha}|_{t_{j-1}}^{t_j}$, and, unsurprisingly, similar instabilities may occur when computing $I_{hist}^{j,\ell}$. We rectify these by splitting $\partial\phi_j^\ell(s)$ in $I_{hist}^{j,\ell}$ as $\partial\phi_j^\ell(t_j) + [\partial\phi_j^\ell(s) - \partial\phi_j^\ell(t_j)]$. Now $I_{hist}^{j,\ell}$ can be split as $\bar{I}_{hist}^{j,\ell} + [I_{hist}^{j,\ell} - \bar{I}_{hist}^{j,\ell}]$, where

$$\begin{aligned} \bar{I}_{hist}^{j,\ell} &:= \partial\phi_j^\ell(t_j) \int_{t_{j-1}}^{t_j} (t - s)^{-\alpha} ds = \frac{\partial\psi^\ell(1)}{(1 - \alpha)\tau_j} (t - s)^{1-\alpha}|_{t_{j-1}}^{t_j} \\ &= \frac{\partial\psi^\ell(1)}{(1 - \alpha)\tau_j} d_{j-1}(t)^{1-\alpha} \text{expm1}((1 - \alpha)\kappa_j(t)). \end{aligned}$$

Here we used $\frac{d}{ds}\phi_j^\ell(t_j) = \tau_j^{-1}\frac{d}{d\sigma}\psi^\ell(1)$ and the stable-implementation formula (19).

For the remaining component $I_{hist}^{j,\ell} - \bar{I}_{hist}^{j,\ell}$ of $I_{hist}^{j,\ell}$ one gets

$$\begin{aligned} I_{hist}^{j,\ell} - \bar{I}_{hist}^{j,\ell} &= \int_{t_{j-1}}^{t_j} [\partial\phi_j^\ell(s) - \partial\phi_j^\ell(t_j)] (t - s)^{-\alpha} ds \\ &= d_{j-1}(t)^{-\alpha} \int_0^1 [\partial\psi^\ell(\sigma) - \partial\psi^\ell(1)] \exp\left(-\alpha \log_{1p}\left(-\frac{\tau_j}{t - t_{j-1}}\sigma\right)\right) d\sigma, \quad (22) \end{aligned}$$

where we used

$$(t - s)^{-\alpha} = (t - t_{j-1} - \tau_j\sigma)^{-\alpha} = d_{j-1}(t)^{-\alpha} \exp\left(-\alpha \log_{1p}\left(-\frac{\tau_j}{t - t_{j-1}}\sigma\right)\right).$$

Note that the above integral is non-singular, as $(t - s)^{-\alpha} \lesssim (t - t_{j-1})^{-\alpha} (1 - \sigma)^{-\alpha}$, while $|\partial\psi^\ell(\sigma) - \partial\psi^\ell(1)| \lesssim 1 - \sigma$. Hence, an adaptive quadrature routine yields a fast and efficient evaluation of the latter integral. For example, we employed `integral` with an appropriate integrand $\chi(\sigma)$ from (22) in the form

$$\text{integral}(@(\sigma)\chi(\sigma), 0, 1, 'ArrayValued', 'true').$$

In addition we supply the options (`'RelTol', 1e-16, 'WayPoints', pts`) with increased relative tolerance for evaluating the integral, and also a hint on how to subdivide the interval of integration in the form of a vector `pts` of sampling points (specified by (24) below). This routine was essential for the evaluation of the residual at sampling points.

To give an example, in our experiments, we used hierarchical basis functions $\{\psi^\ell\}_{\ell \in \{0, \dots, m\}}$ defined by

$$\psi^0(\sigma) := 1 - \sigma, \quad \psi^m(\sigma) := \sigma, \quad \psi^\ell(\sigma) := \sigma^\ell(1 - \sigma) \quad \forall \ell \in \{1, \dots, m - 1\}. \quad (23)$$

Then $-\partial\psi^0(\sigma) = \partial\psi^m(\sigma) = 1$, and for $\ell \in \{1, \dots, m-1\}$ from $\partial\psi^\ell(\sigma) = \ell\sigma^{\ell-1}(1-\sigma) - \sigma^\ell$ one easily gets

$$\partial\psi^\ell(1) = -1, \quad 0 \leq \partial\psi^\ell(\sigma) - \partial\psi^\ell(1) = \ell\sigma^{\ell-1}(1-\sigma) - \sigma^\ell + 1 \lesssim 1 - \sigma.$$

The remaining integral I_{sing}^ℓ is singular, but can be evaluated analytically as follows. A transformation using (21) and $t_{loc} := \frac{t-t_{k-1}}{\tau_k}$ yields $(t-s)^{-\alpha} = (t-t_{k-1}-\tau_k\sigma)^{-\alpha} = \tau_k^{-\alpha}(t_{loc}-\sigma)^{-\alpha}$, and then

$$I_{sing}^\ell = \tau_k^{-\alpha} \int_0^{t_{loc}} \partial\psi^\ell(\sigma) (t_{loc}-\sigma)^{-\alpha} d\sigma =: \tau_k^{-\alpha} \hat{I}_{sing}^\ell.$$

We observe, that the evaluation is reduced to finding an integral $\hat{I}_{sing}^\ell = \hat{I}_{sing}^\ell(t_{loc})$ that depends only on t_{loc} . For example, with our choice (23), a calculation yields

$$\begin{aligned} \hat{I}_{sing}^m &= -\hat{I}_{sing}^0 = t_{loc}^{1-\alpha} \cdot \frac{1}{1-\alpha}, \\ \hat{I}_{sing}^1 &= t_{loc}^{1-\alpha} \cdot \frac{2t_{loc} - (2-\alpha)}{(1-\alpha)(2-\alpha)}, \end{aligned}$$

while \hat{I}_{sing}^ℓ for other values of ℓ can be easily evaluated in a similar way. Furthermore, the sampling points for the evaluation of the residuals on each $[t_{k-1}, t_k]$ are typically chosen as $t = t_{k-1} + \tau_k t_{loc}$, where t_{loc} takes values from a certain predefined set; hence, all $m+1$ integrals $\hat{I}_{sing}^\ell(t_{loc})$ can be pre-computed offline for all ℓ and all t_{loc} of interest. For the L1-2 method we obtain by the same reasoning the stable formulation

$$\begin{aligned} D_t^\alpha u_h(t) &= \frac{1}{\Gamma(2-\alpha)} \sum_{j=1}^{k-1} -\frac{U_j - U_{j-1}}{\tau_j} d_{j-1}(t)^{1-\alpha} \text{expm1}((1-\alpha)\kappa_j(t)) \\ &\quad + \frac{1}{\Gamma(2-\alpha)} \sum_{j=2}^{k-1} y_j \tau_j d_{j-1}(t)^{1-\alpha} \text{expm1}((1-\alpha)\kappa_j(t)) \\ &\quad + \frac{2}{\Gamma(1-\alpha)} \sum_{j=2}^{k-1} y_j \tau_j^2 d_{j-1}(t)^{-\alpha} \int_0^1 (\sigma-1) \exp\left(-\alpha \log_{1p}\left(-\frac{\tau_j}{t-t_{j-1}}\sigma\right)\right) d\sigma \\ &\quad + \frac{1}{\Gamma(1-\alpha)} \left((U_k - U_{k-1}) \tau_k^{-\alpha} (-\hat{I}_{sing}^0) + y_k \tau_k^{2-\alpha} \hat{I}_{sing}^1 \right), \end{aligned}$$

where \hat{I}_{sing}^0 and \hat{I}_{sing}^1 are as above. Note that the parts without y are exactly the same as for the L1 method.

Sampling points

On each interval, the residuals R_h (and, hence, $D_t^\alpha u_h$) were evaluated using

$$t_{loc} \in \left\{ \left(\frac{i}{n} \right)^p \right\} \quad \text{for } i \in \{1, \dots, n-1\}, \quad (24)$$

i.e. this set forms a graded grid on $[0, 1]$. In our computations, we set $n + 1 := 21$ and heuristically choose the grading exponent $p := \min\{\frac{1}{1-\alpha}, 5\}$, which gives a sufficiently strong sampling near the maximal residual values, as we shall now discuss.

Indeed, for our algorithm to be reliable, it is essential that the set of sampling points reaches the maximal value of the residual, while the residual itself behaves on each $[t_{k-1}, t_k]$ like a left-shifted bubble with a sharp layer near t_{k-1} as $\alpha \rightarrow 1^-$. The latter behaviour is easily understood, e.g., in the case of the L1 method, as in the extreme case $\alpha = 1$, the residual involves a piecewise-constant $D_t^\alpha u_h = \frac{d}{dt}u_h$ and, thus, has discontinuities at each t_{k-1}^+ . With above choice of p and n , we observe a good distribution of sampling points as shown in Fig. 5. catching the maximum value. Interestingly, for $\alpha = 0.1$ we also observe a sharp layer in the residual bubble, but now only for a few initial time intervals.

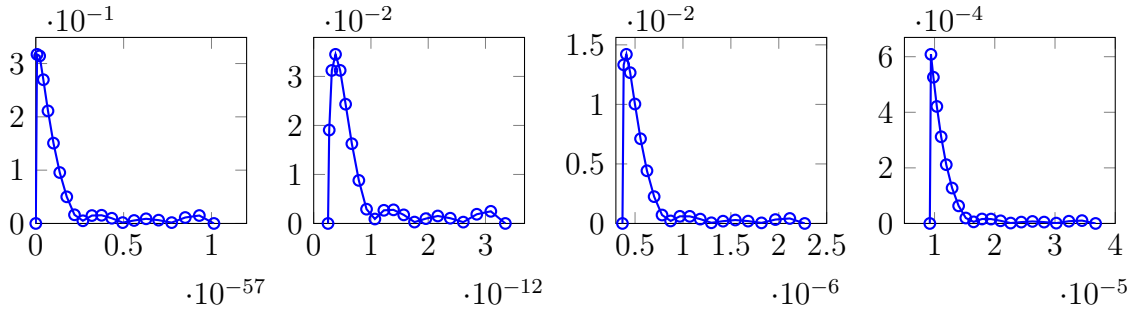


Figure 5: Distribution of sampling points for a collocation method with $m = 4$ inside the second interval for $\alpha \in \{0.1, 0.4, 0.8, 0.99\}$ (from left to right)

5 Adaptive algorithm

Here we present a version of the adaptive time stepping algorithm from [10, 12], in which we made a few subtle improvements that substantially reduce the computational time; see Algorithm 1.

Our algorithm yields a mesh with mesh nodes $\{t_j\}$, such that $0 = t_0 < t_1 < \dots < t_M = T$ (where a suitable M is chosen by the algorithm) and a computed solution on this mesh, such that the residual of the computed solution, measured in the $L_p(\Omega)$ norm, does not exceed $TOL \cdot \mathcal{R}_0(t)$ or $TOL \cdot \mathcal{R}_1(t)$, the residual barriers suggested by (8), or, equivalently, by (9). Similarly to [10, 12], the algorithm calls three functions:

- `computeSolution(mesh,oldSolution)` that employs a numerical method from Section 3 to compute the solution $u_h|_{(t_{m-1},t_m]}$ using a given mesh $\{t_j\}_{j=0}^m$ and the solution $u_h|_{[0,t_{m-1}]}$ as initial data;
- `computeResidual(solution,mesh)` that computes the $L_p(\Omega)$ -norm of the residual (as described in Section 3.4) at the prescribed set of sampling points in $(t_{m-1}, t_m]$ using a given mesh $\{t_j\}_{j=0}^m$ and the solution $u_h|_{[0,t_m]}$ as initial data;

Algorithm 1: Adaptive Algorithm

```

1 m      := 1;
2 Q      := Q0;
3 uh(1)  := u0;
4 mesh(1:2) := [0, tau_init];
5 while mesh(m) < T
6     if (m=2 && Q=Q0)                                % found initial guess for mesh(1)
7         Q := Q1;
8     else
9         m := m+1;
10    end
11    flag := 0;
12    while mesh(m) - mesh(m-1) > tau_min
13        uh(m) := computeSolution(mesh(1:m), uh);
14        Res   := computeResidual(uh, mesh);
15        ResBarrier := computeResidualBarrier(mesh);
16        if all(Res < TOL * ResBarrier)                % residual small enough
17            if mesh(m) >= T                            % finished
18                break
19            else                                        % ok
20                if flag = 2                            % coming from larger stepsizes
21                    mesh(m+1) := min(mesh(m) + (mesh(m) - mesh(m-1)), T);
22                    break;                            % continue with next step
23                end
24                tmpuh := uh(m);                        % save data
25                tmptm := mesh(m);
26                mesh(m) := min(mesh(m-1) + Q * (mesh(m) - mesh(m-1)), T);
27                flag := 1;                            % try again with larger step
28            end
29            else                                        % residual not small enough
30                if flag = 1                            % previous step was good
31                    uh(m) := tmpuh;                  % recall saved data
32                    mesh(m) := tmptm;
33                    mesh(m+1) := min(mesh(m) + (mesh(m) - mesh(m-1)), T);
34                    break;                            % continue with next step
35                else                                    % previous residual not good
36                    mesh(m) := mesh(m-1) + (mesh(m) - mesh(m-1)) / Q;
37                    flag := 2;                        % try again with smaller step
38                end
39            end
40        end
41        if mesh(m) - mesh(m-1) < tau_min
42            mesh(m) := min(mesh(m-1) + tau_min, T);
43            mesh(m+1) := min(mesh(m-1) + 2 * tau_min, T);
44        end
45    end

```

- `computeResidualBarrier(mesh)` that computes the barriers \mathcal{R}_0 or \mathcal{R}_1 at the prescribed set of sampling points on $(t_{m-1}, t_m]$.

Furthermore, the following parameters are used

- TOL is a sufficiently small positive number used in the guaranteed estimate for the error of the computed solution.
- $\tau_{init} = T/2$ is a very crude initial guess for the first time step τ_1 . This will typically be shrunk by the factor Q_0 (see below) in the first few iterations.
- $\tau_{min} \geq 0$ is the lower bound on any time step enforced by the algorithm. We set it to 0, but the algorithm allows for any small positive value.
- $Q_0 > Q_1 > 1$ are two factors by which the size of the current time step is increased or reduced. Here the larger factor Q_0 is used to find a crude size for the starting time step τ_1 , while the smaller factor $Q_1 \approx 1$ is used to find the final size of τ_1 , as well as to compute all other time steps. In our experiments we chose $Q_0 = 5$ and the initial search was done within 10 iterations.

Note that, compared to [10, 12], the introduction of the larger factor Q_0 (used to compute a crude size of τ_1), as well as **flag** = 2, significantly reduces the computational times.

Remark 5.1 ($\omega > 0$). *Note that when the bounds of Corollary 2.9 are employed, in view of (10) (used instead of (9)), the residual of the computed solution, measured in the $L_\infty(\Omega)$ norm, should not exceed $TOL \cdot \mathcal{R}_0(t)/(1 + \omega)$ or $TOL \cdot \mathcal{R}_1(t)/(1 + \omega)$, which requires an obvious minor change in line 15 of the algorithm to*

$$\text{ResBarrier} := \text{computeResidualBarrier}(\text{mesh})/(1+\omega);$$

6 Numerical experiments

We are mainly interested in the adaptive time stepping and, therefore, we consider only simple problems in the spatial direction. We use a conforming finite element method with piecewise polynomials of a fixed degree in space on a sufficiently fine equidistant mesh. For simplicity, throughout this Section, all test problems posed in $(0, T] \times \Omega$ will be of the form

$$D_t^\alpha u - \Delta u = f,$$

subject to homogeneous boundary conditions.

Example 6.1: In order to compare the residual to the actual error we consider a test problem with a given exact solution. Here we take $\Omega = (0, 1)$ and

$$u(x, t) = (t^\alpha - t^2 + 1)x(1 - x)$$

that satisfies the homogeneous boundary conditions and the initial condition with $u_0(x) = x(1 - x)$, and exhibits a typical weak singularity of type t^α near $t = 0$. Note that the

solution is a quadratic polynomial in space for each $t \geq 0$. Therefore, using piecewise quadratic elements in space, on a coarse spatial grid of just 10 cells, resolves it exactly and the error obtained is purely due to time discretisation.

Example 6.2: In order to investigate the behaviour of the adaptive algorithm and its parameters we consider a second test problem with an unknown solution posed in $\Omega = (0, 1)$, but a given right-hand side

$$f(x, t) = (t^\gamma - t) \cdot \sin((x\pi)^2) + t \cdot \exp(-100 \cdot (2t - 1)^2)$$

for $\gamma \in [0, \alpha]$. Note, that this function has a very localised Gaussian pulse in addition to the weak singularity of type $t^{\gamma+\alpha}$ near $t = 0$. The solution of this problem for $\alpha = 0.4$ is shown in Figure 6 for $0 \leq t \leq 1$. Note that similar problems posed in $\Omega = [0, 1]^d$ for $d \in \{2, 3\}$

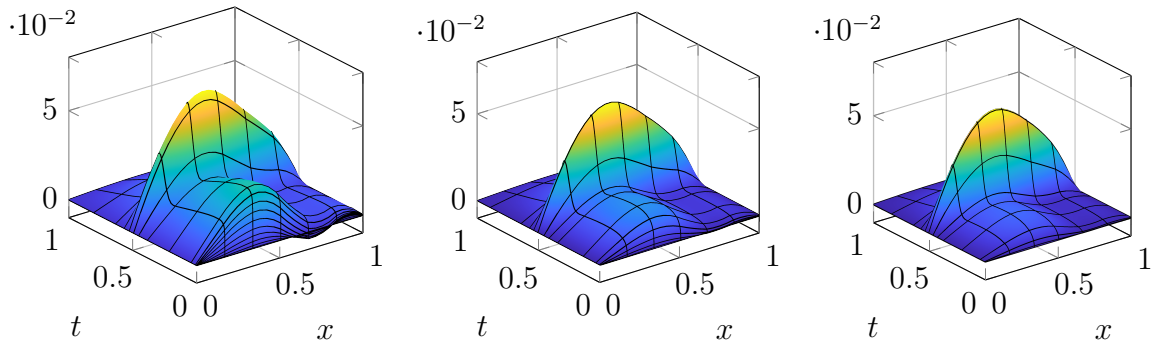


Figure 6: Solution of Example 6.2 with $\alpha = 0.4$ and $\gamma \in \{0, 0.2, 0.4\}$ from left to right

were also investigated with similar results. For the spatial discretisation we use the same method as before and apply piecewise quadratic elements on a spatial grid of 10 cells.

6.1 Experiments on the reliability and convergence rates with Example 6.1

Let us start by investigating the reliability of our error estimator using Example 6.1, for which the exact solution is available. For the mesh adaptation process we use $Q_1 = 1.2$ unless specified otherwise. Recall that for this problem, in view of Lemma 2.5 combined with Remark 2.6(ii), one can employ $\omega = \frac{1}{8}\lambda$ for any $\lambda \geq 0$ when measuring the error in the $L_\infty(\Omega)$ norm (see also Remark 5.1 for this case). When the error is measured in the $L_2(\Omega)$ norm, the principal eigenvalue $\lambda = \pi^2$ of the operator $L = -\partial_x^2$ on $\Omega = (0, 1)$ satisfies Theorem 2.1, so will be used in \mathcal{R}_0 and \mathcal{R}_1 .

Figures 7–12 show loglog graphs of various values of the algorithm's TOL and the corresponding actual errors vs. the corresponding numbers of time steps M (recall that M is automatically chosen by the algorithm for a prescribed value of TOL). The L1 method, the L1-2 method, and a few collocation methods up to order $m = 8$ are considered. Given a method of order q , we expect convergence rates of order $q - \alpha$ (see Remark 2.10). Hence, we also show the slopes for $M^{-(2-\alpha)}$ and $M^{-(5-\alpha)}$, which are, respectively, expected to have

a good agreement with the error curves for the L1 method and the collocation method of order $m = 4$. (The slope for $m = 8$ is not given, as the prescribed tolerance TOL is attained while we remain in a preasymptotic regime, with very few time steps M .)

We start with the residual barrier \mathcal{R}_0 , with $\lambda = \pi^2$ and $\omega = \lambda/8$, and measure the error in the $L_\infty(0, T; L_\infty(\Omega))$ norm; see Figure 7. We clearly observe a tight bounding of the errors

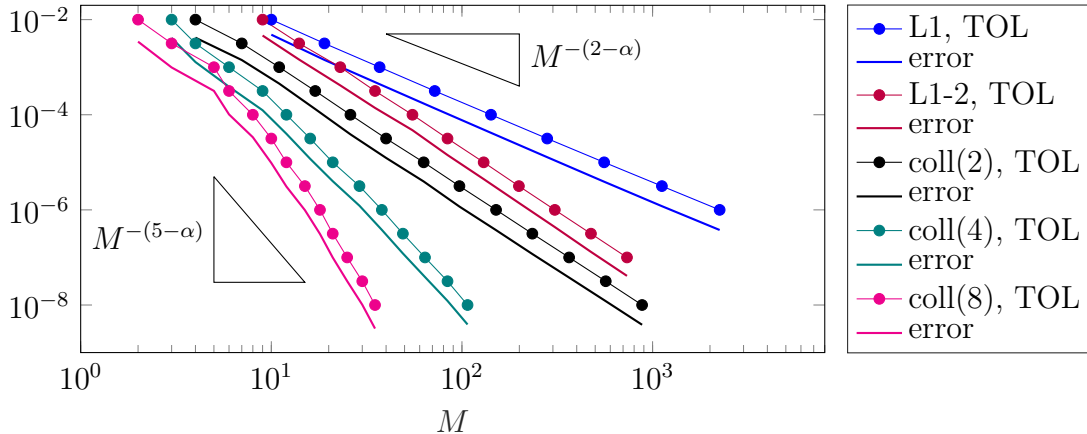


Figure 7: $L_\infty(0, T; L_\infty(\Omega))$ errors for various methods vs. number of time steps M for Example 6.1, $\alpha = 0.4$, residual barrier \mathcal{R}_0 with $\lambda = \pi^2$ and $\omega = \lambda/8$

by the prescribed values of TOL and therefore a good demonstration of the reliability of the estimator. Furthermore, we observe convergence orders of almost $\mathcal{O}(M^{-(q-\alpha)})$, where $q = 2$ for the L1 method, $q = 3$ for the L1-2 method, and $q = m + 1$, where m is the polynomial degree used in the definition of the collocation methods in Section 3.3. Note that there are no theoretical a-priori error estimates in the literature for the considered collocation methods in the context of our problem (1), while our adaptive algorithm yields reliable computed solutions with optimal convergence rates.

Figure 8 shows the results for the same problem, but now we choose $\lambda = 0$ and $\omega = 0$. We observe a tighter fit of the error to the corresponding TOL , but at the same time for the lower-order methods more time steps were required by the algorithm in comparison to the previous choice of λ and ω .

Changing the spatial norm to $L_2(\Omega)$, we observe a similar behaviour in the adaptivity and convergence; see Figure 9.

For smaller values of α the singularity at $t = 0$ is stronger (assuming it is of type t^α , as discussed in Remark 2.10), so we observe a stronger initial mesh refinement, as is also illustrated by Figure 5. At the same time, Figure 10 shows that the mesh adaptation process works similarly well for $\alpha = 0.1$. But for really small α we run into numerical issues. For example, $\alpha = 0.01$ and $TOL = 10^{-3}$ for the collocation method with $m = 4$ yield the first time step $\tau_1 \approx 1.2 \cdot 10^{-270}$ (which is consistent with $\tau_1 = M^{-r}$ for the optimal graded mesh with $r = (m + 1 - \alpha)/\alpha$; see, e.g., [11]). For smaller values of TOL , higher m , and/or smaller α , the size of τ_1 becomes numerically zero, as the smallest positive number in MatLab is $2^{-1074} \approx 5 \cdot 10^{-324}$. In other words, for very small α , double precision is no longer sufficient to represent the first time step.

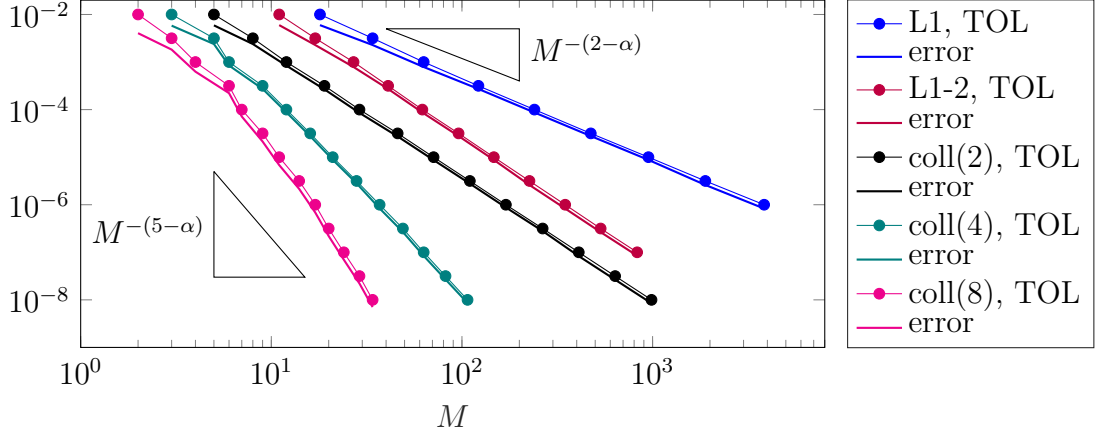


Figure 8: $L_\infty(0, T; L_\infty(\Omega))$ errors for various methods vs. number of time steps M for Example 6.1, $\alpha = 0.4$, residual barrier \mathcal{R}_0 with $\lambda = \omega = 0$

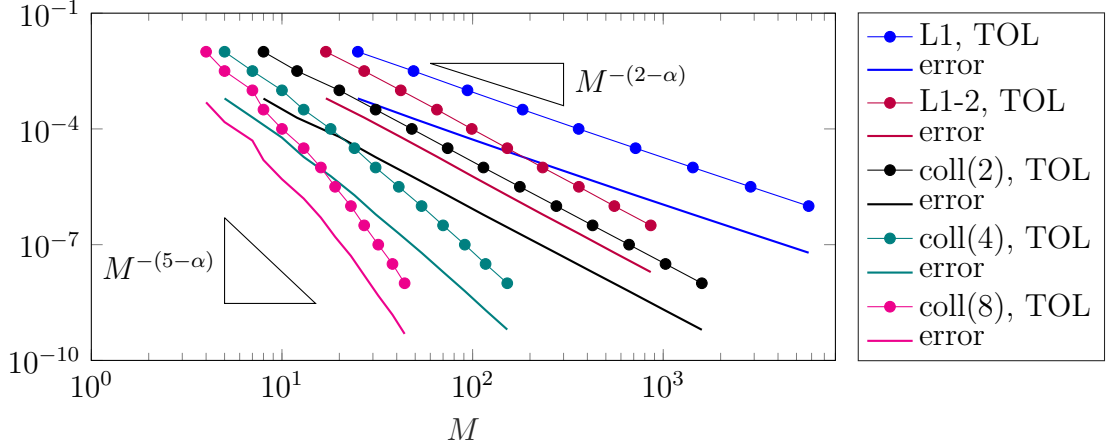


Figure 9: $L_\infty(0, T; L_2(\Omega))$ errors for various methods vs. number of time steps M for Example 6.1, $\alpha = 0.4$, residual barrier \mathcal{R}_0 with $\lambda = \pi^2$

For higher values of α the singularity at $t = 0$ is weaker, but the residuals become more singular (see Figure 5). Figure 11 shows in the case $\alpha = 0.8$ that the mesh adaptation process works similarly well in this regime. In fact, we tested the algorithm for values of up to $\alpha = 0.999$ and observed consistently good convergence behaviour.

With the help of the second residual barrier \mathcal{R}_1 , we can bound the error at a given final time, here $T = 1$, while employing a weaker mesh refinement (as the resulting error is guaranteed to be bounded by $TOL \cdot t^{\alpha-1}$). Figure 12 shows the results for $\alpha = 0.4$. We observe, that the error behaviour is not as smooth as for the other estimator for higher-order methods. This is partially caused by $Q_1 = 1.2$, while we remain in a preasymptotic regime, with very few time steps M required by the adaptive algorithm (Q_1 closer to 1 would produce smoother error curves, but would require more iterations; see Figure 16 below).

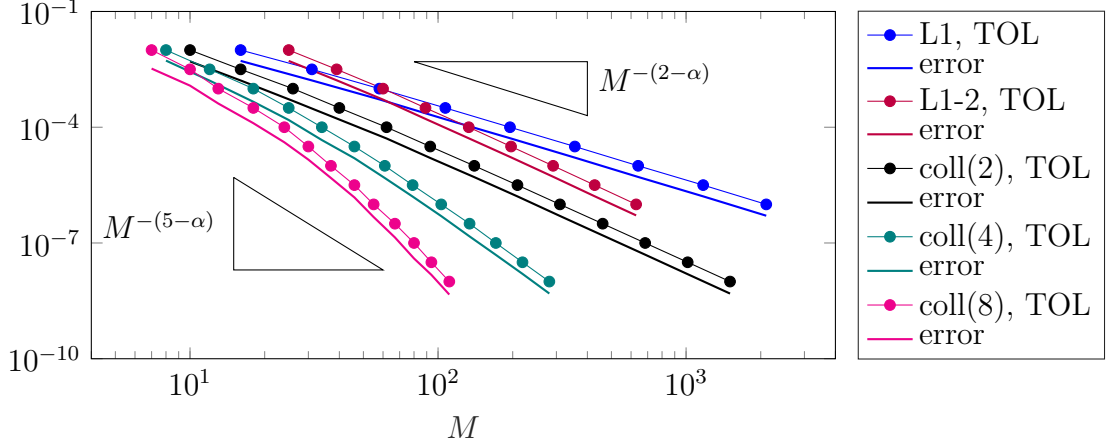


Figure 10: $L_\infty(0, T; L_\infty(\Omega))$ errors for various methods vs. number of time steps M for Example 6.1, $\alpha = 0.1$, residual barrier \mathcal{R}_0 with $\lambda = \pi^2$ and $\omega = \lambda/8$

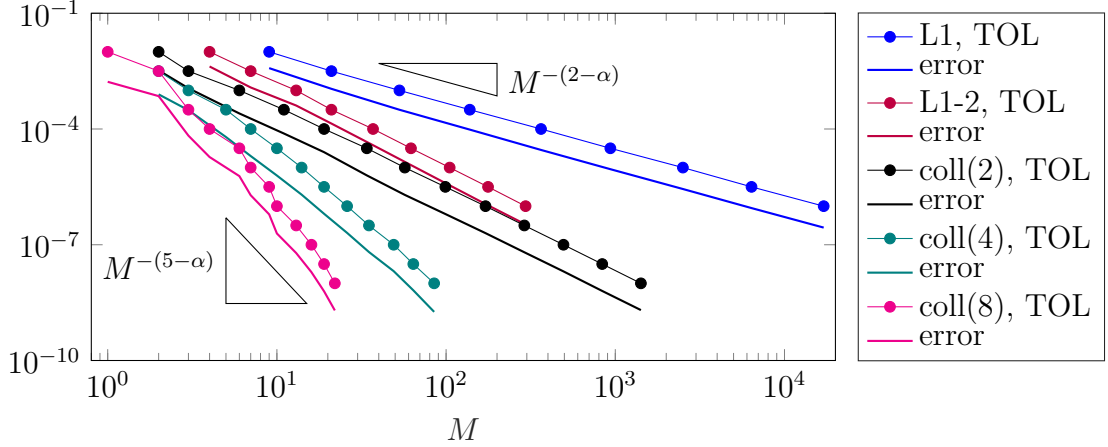


Figure 11: $L_\infty(0, T; L_\infty(\Omega))$ errors for various methods vs. number of time steps M for Example 6.1, $\alpha = 0.8$, residual barrier \mathcal{R}_0 with $\lambda = \pi^2$ and $\omega = \lambda/8$

6.2 Experiments with Example 6.2. Algorithm parameters

The purpose of this section is twofold. First, experiments with Example 6.2, with an unknown solution that exhibits an initial weak singularity at $t = 0$ (depending on γ) and a localised Gaussian pulse near $t = 0.5$ (see Figure 6) will illustrate that our algorithm is capable of adapting the temporal mesh to various solution singularities. Second, we will numerically investigate the parameters of the adaptive algorithm, in view of computational costs vs. the resulting errors. Thus, throughout this section, we apply our algorithm to Example 6.2 using the residual barrier \mathcal{R}_0 with the $L_\infty(\Omega)$ norm and $\lambda = \pi^2$, $w = \lambda/8$.

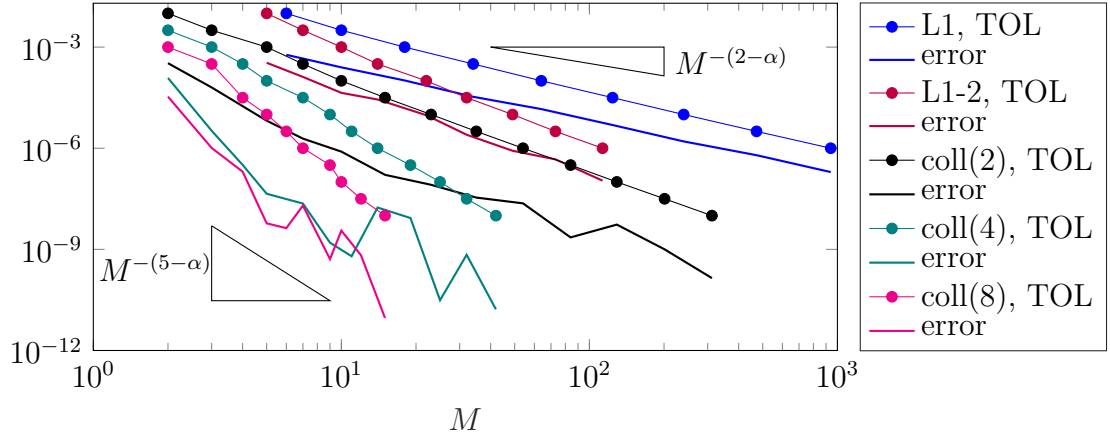


Figure 12: $L_\infty(\Omega)$ errors at $T = 1$ for various methods vs. number of time steps M for Example 6.1, $\alpha = 0.4$, residual barrier \mathcal{R}_1 with $\lambda = \pi^2$ and $\omega = \lambda/8$

Adaptivity for various solution singularities

Set $\alpha = 0.4$ and $\gamma = 0$ in Example 6.2. The adaptive time stepping was applied with $TOL = 10^{-4}$, $Q_1 = 1.2$, for the collocation methods of order $m \in \{1, 2, 4, 8\}$ (which includes the L1-method for $m = 1$), with the generated time steps shown in Figure 13. We see, that

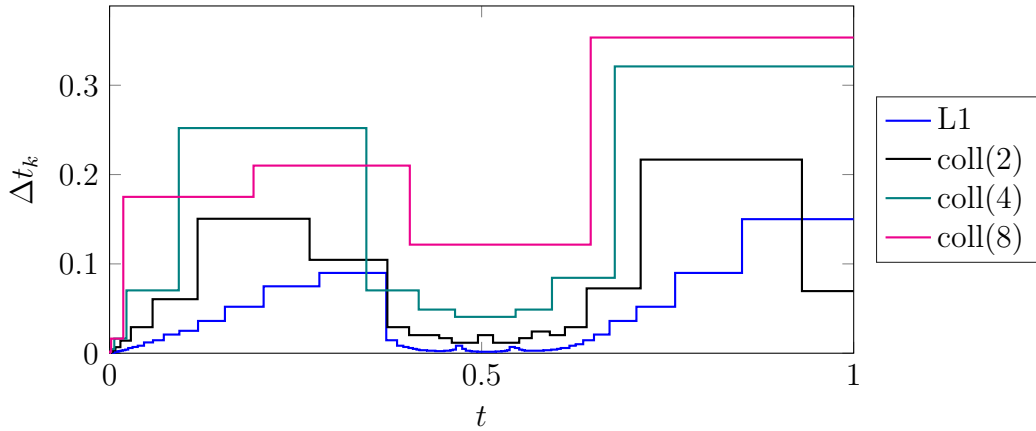


Figure 13: Time steps vs. time for 4 collocation methods applied to Example 6.2, $\alpha = 0.4$, $\gamma = 0$, $Q_1 = 1.2$, $TOL = 10^{-4}$, residual barrier \mathcal{R}_0 with $L_\infty(\Omega)$ norm and $\lambda = \pi^2$, $w = \lambda/8$

indeed the meshes are refined near the two problematic points with a finer mesh for lower-order methods like the L1 method. We also considered $\alpha = 0.8$ and varied $\gamma \in [0, \alpha]$. The adaptivity to the initial singularity of type $t^{\gamma+\alpha}$ as γ changes is clearly shown in Figure 14. Note also that when the solution is of type t^α , the adaptive temporal mesh becomes similar to the optimal graded mesh, described in Remark 2.10, as is more clearly shown in [10, Fig. 1].

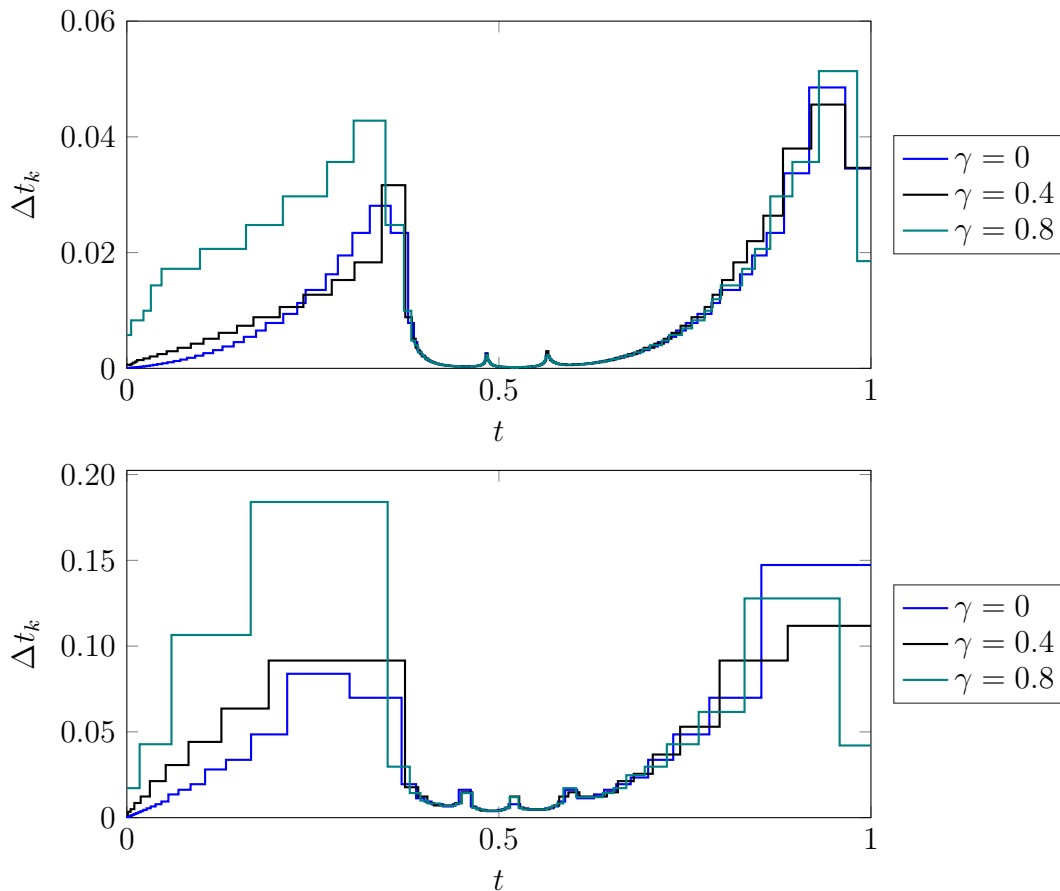


Figure 14: Time steps vs. time for Example 6.2 for varying γ and the L1 method (top) and coll(2) (bottom), $\alpha = 0.8$, $Q_1 = 1.2$, $TOL = 10^{-4}$, residual barrier \mathcal{R}_0 with $L_\infty(\Omega)$ norm and $\lambda = \pi^2$, $w = \lambda/8$

Parameter Q_1

Next, we want to investigate the influence of the value of $Q_1 > 1$ on the number of time steps. In Figure 15 we see for $m \in \{1, 2, 4, 8\}$ the number of time steps M in the adaptively-generated mesh for varying values of Q_1 . We observe that the number of time steps increases with increasing Q_1 , but very moderately in general, and even more so for higher-order methods. Thus, for an optimal mesh a relatively small value of $Q_1 > 1$ should be taken. On the other hand, smaller values of Q_1 may lead to many iterations and, therefore, higher computational costs, as shown in Figure 16. We observe a drastic increase of algorithm iterations, and, hence, computational time and costs for as Q_1 becomes close to 1.

- We conclude that a small value of $Q_1 = 1.1$ or $Q_1 = 1.2$ seems to be a good compromise between computational costs and quality of the mesh.
- A higher order method leads to a much smaller number of time steps at similar costs for adapting the mesh.

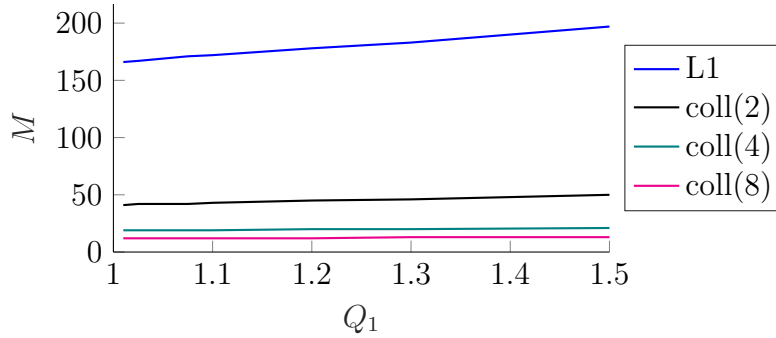


Figure 15: Number of time intervals M vs. Q_1 for 4 collocation methods applied to Example 6.2, $\alpha = 0.4$, $\gamma = 0$, $TOL = 10^{-4}$, residual barrier \mathcal{R}_0 with $L_\infty(\Omega)$ norm and $\lambda = \pi^2$, $w = \lambda/8$

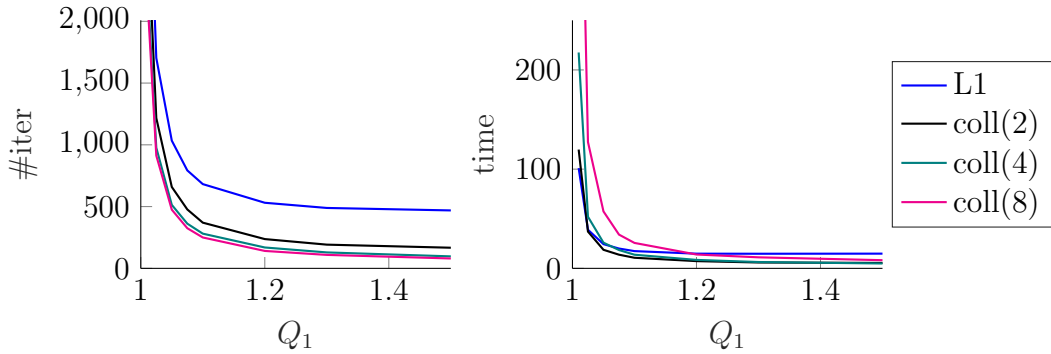


Figure 16: Computational costs vs. Q_1 for 4 collocation methods applied to Example 6.2, $\alpha = 0.4$, $\gamma = 0$, $TOL = 10^{-4}$, residual barrier \mathcal{R}_0 with $L_\infty(\Omega)$ norm and $\lambda = \pi^2$, $w = \lambda/8$

Figure 17 shows the number of iterations and the corresponding computational time for varying values of TOL and fixed $Q_1 = 1.2$. As to be expected, smaller values of TOL yield smaller errors, but lead to higher computational costs. This is even stronger observable for the lowest-order method.

- For a given value of TOL , higher-order method are less costly.

Finally, Figure 18 shows the behaviour of the residuals. The upper bound of (9a), imposed on the residual by the algorithm, is depicted in black, and, as expected, all residuals are below this bound.

7 Conclusions

Time-fractional parabolic equations with a Caputo time derivative were considered. For such equations, we have reviewed and generalized the a-posteriori error estimates from [10], and improved the earlier time stepping algorithm based on this theory. A number of temporal discretizations were considered, including the L1 method, an L1-2 method, and continuous

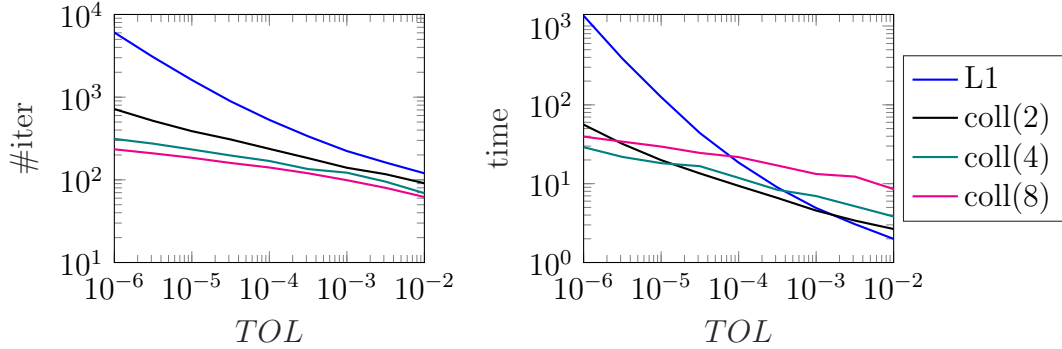


Figure 17: Computational costs vs. TOL for 4 collocation methods applied to Example 6.2, $\alpha = 0.4$, $\gamma = 0$, $Q_1 = 1.2$, residual barrier \mathcal{R}_0 with $L_\infty(\Omega)$ norm and $\lambda = \pi^2$, $w = \lambda/8$

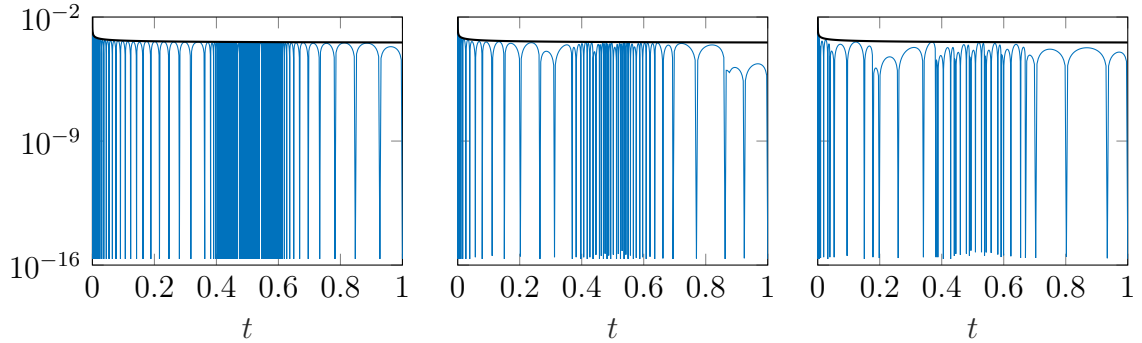


Figure 18: Residuals and the algorithm's residual bounds for collocation methods of order $m \in \{1, 2, 4\}$ (left to right) applied to Example 6.2, $\alpha = 0.4$, $\gamma = 0$, $Q_1 = 1.2$, $TOL = 10^{-4}$, residual barrier \mathcal{R}_0 with $L_\infty(\Omega)$ norm and $\lambda = \pi^2$, $w = \lambda/8$

collocation methods of arbitrary order. A stable and efficient implementation of the resulting algorithm was described, which is essential in the context of higher-order methods. It was demonstrated that high-order methods (of order up to as high as 8) exhibit a huge improvement in the accuracy when the time steps are chosen adaptively, and, furthermore, adaptive temporal meshes yield optimal convergence rates in the presence of various solution singularities.

Funding

The second author was partially supported by Science Foundation Ireland under Grant number 18/CRT/6049.

References

- [1] Lehel Banjai and Charalambos G. Makridakis. A posteriori error analysis for approximations of time-fractional subdiffusion problems. *Math. Comp.*, 91(336):1711–1737,

2022.

- [2] Hermann Brunner. *Collocation methods for Volterra integral and related functional differential equations*, volume 15 of *Cambridge Monographs on Applied and Computational Mathematics*. Cambridge University Press, Cambridge, 2004.
- [3] Kai Diethelm. *The analysis of fractional differential equations*, volume 2004 of *Lecture Notes in Mathematics*. Springer-Verlag, Berlin, 2010. An application-oriented exposition using differential operators of Caputo type.
- [4] Lawrence C. Evans. *Partial differential equations*, volume 19 of *Graduate Studies in Mathematics*. American Mathematical Society, Providence, RI, second edition, 2010.
- [5] Guang-hua Gao, Zhi-zhong Sun, and Hong-wei Zhang. A new fractional numerical differentiation formula to approximate the Caputo fractional derivative and its applications. *J. Comput. Phys.*, 259:33–50, 2014.
- [6] Bangti Jin, Raytcho Lazarov, and Zhi Zhou. Numerical methods for time-fractional evolution equations with nonsmooth data: a concise overview. *Comput. Methods Appl. Mech. Engrg.*, 346:332–358, 2019.
- [7] Natalia Kopteva. Error analysis of the L1 method on graded and uniform meshes for a fractional-derivative problem in two and three dimensions. *Math. Comp.*, 88(319):2135–2155, 2019.
- [8] Natalia Kopteva. Error analysis of an L2-type method on graded meshes for a fractional-order parabolic problem. *Math. Comp.*, 90(327):19–40, 2021.
- [9] Natalia Kopteva. Maximum principle for time-fractional parabolic equations with a reaction coefficient of arbitrary sign. *Appl. Math. Lett.*, 132:Paper No. 108209, 7, 2022.
- [10] Natalia Kopteva. Pointwise-in-time a posteriori error control for time-fractional parabolic equations. *Appl. Math. Lett.*, 123:Paper No. 107515, 8, 2022.
- [11] Natalia Kopteva and Xiangyun Meng. Error analysis for a fractional-derivative parabolic problem on quasi-graded meshes using barrier functions. *SIAM J. Numer. Anal.*, 58(2):1217–1238, 2020.
- [12] Natalia Kopteva and Martin Stynes. A Posteriori Error Analysis for Variable-Coefficient Multiterm Time-Fractional Subdiffusion Equations. *J. Sci. Comput.*, 92(2):Paper No. 73, 2022.
- [13] Hong-lin Liao, Dongfang Li, and Jiwei Zhang. Sharp error estimate of the nonuniform L1 formula for linear reaction-subdiffusion equations. *SIAM J. Numer. Anal.*, 56(2):1112–1133, 2018.
- [14] Hong-lin Liao, Dongfang Li, and Jiwei Zhang. Sharp error estimate of the nonuniform L1 formula for linear reaction-subdiffusion equations. *SIAM J. Numer. Anal.*, 56(2):1112–1133, 2018.

- [15] Yuri Luchko and Masahiro Yamamoto. On the maximum principle for a time-fractional diffusion equation. *Fract. Calc. Appl. Anal.*, 20(5):1131–1145, 2017.
- [16] Chunwan Lv and Chuanju Xu. Error analysis of a high order method for time-fractional diffusion equations. *SIAM J. Sci. Comput.*, 38(5):A2699–A2724, 2016.
- [17] William McLean. Implementation of high-order, discontinuous Galerkin time stepping for fractional diffusion problems. *The ANZIAM Journal*, 62(2):121–147, 2020.
- [18] Lawrence F. Shampine. Vectorized adaptive quadrature in Matlab. *J. Comput. Appl. Math.*, 211(2):131–140, 2008.
- [19] Martin Stynes. A survey of the L1 scheme in the discretisation of time-fractional problems. 10.13140/RG.2.2.27671.60322.
- [20] Martin Stynes, Eugene O’Riordan, and José Luis Gracia. Error analysis of a finite difference method on graded meshes for a time-fractional diffusion equation. *SIAM J. Numer. Anal.*, 55(2):1057–1079, 2017.